Draft version February 2, 2008
Preprint typeset using LaTeX style emulateapj v. 02/09/03

GRAVITATIONAL LENSING OF THE MICROWAVE BACKGROUND BY GALAXY CLUSTERS

Gilbert Holder
School of Natural Sciences, Institute for Advanced Study, Einstein Drive, Princeton, NJ 08540

Arthur Kosowsky
Department of Physics and Astronomy, Rutgers University, 136 Frelinghuysen Road, Piscataway, NJ 08854-8019
Draft version February 2, 2008

ABSTRACT

Galaxy clusters will distort the pattern of temperature anisotropies in the microwave background via gravitational lensing. We create lensed microwave background maps using clusters drawn from numerical cosmological simulations. A distinctive dipole-like temperature fluctuation pattern is formed aligned with the underlying microwave temperature gradient. For a massive cluster, the characteristic angular size of the temperature distortion is a few arcminutes and the characteristic amplitude a few micro-Kelvin. We demonstrate a simple technique for estimating the lensing deflection induced by the cluster; microwave background lensing measurements have the potential to determine the mass distribution for some clusters with good accuracy on angular scales up to a few arcminutes. Future high-resolution and high-sensitivity microwave background maps will have the capability to detect lensing by clusters; we discuss various systematic limitations on probing cluster masses using this technique.

Subject headings: cosmology: theory – galaxies: clusters: general – cosmic microwave background – gravitational lensing

1. introduction

In the post-WMAP era of microwave background measurements, attention is quickly shifting to smaller angular scales. At scales below 4 arcminutes, the temperature fluctuations are dominated not by primordial fluctuations associated with the last scattering surface but rather by secondary fluctuations induced by interactions with the matter distribution at lower redshifts. Most prominent among these effects are the Sunyaev-Zeldovich effect (Sunyaev & Zel'dovich 1972) and gravitational lensing.

This paper studies the gravitational lensing of the microwave background by galaxy clusters. Much recent effort has been devoted to lensing of the microwave background by the large-scale distribution of matter (Hirata & Seljak 2003; Kesden et al. 2003; Okamoto & Hu 2002, 2003), and lensing of optical and radio sources by galaxies, galaxy clusters, and large-scale structure is a major theoretical and experimental industry. Curiously, little effort so far has been put into lensing of the microwave background by clusters; the only major work on the subject is the seminal paper by Seljak & Zaldarriaga (2000). The likely reason for this benign neglect is that only recently have microwave maps of sufficient resolution and sensitivity to detect cluster lensing become a realistic expectation (Kosowsky 2003; Wootten 2002). The subject has recently been taken up by Dodelson & Starkman (2003) as it relates to galaxies; Cooray (2003) explicitly showed the dependence of the lensing signal on cosmological parameters, and Bartelmann (2003) showed a map of a cluster lensing the CMB as an application of numerical techniques for gravitational lensing.

Observing cluster lensing of the cosmic microwave background requires temperature variations on scales large compared to the cluster (so that we have something to lens), but minimal variations on scales comparable to the size of the cluster (so that the lensing signal can be cleanly separated from the intrinsic temperature fluctuations). Notably, this is exactly what the primary microwave background fluctuations offer. A microwave background temperature map is dominated by fluctuations on scales of a degree or larger, arising from density and temperature perturbations at the surface of last scattering at a redshift $z \simeq 1100$. At scales smaller than a degree, the power spectrum of temperature fluctuations begins to decline due to diffusion damping: perturbations on scales smaller than the thickness of the last scattering surface are exponentially suppressed. On typical cluster angular scales of a few arcminutes, the primordial temperature perturbations are negligible. Secondary, nonlinear temperature fluctuations will arise, but these are generally either tiny (e.g., gravitational lensing by large-scale structure) or have a frequency dependence different from the blackbody distortions due to lensing (e.g. the thermal Sunyaev-Zeldovich effect). The only source of significant nearly-blackbody fluctuations on scales of galaxy clusters besides lensing is the kinematic Sunyaev-Zeldovich distortion, mainly due to the peculiar motion of the cluster itself as well as a small component from large scale structure (Vishniac 1987). In general, the kSZ signal has a different morphology than the lensing signal, and in most cases the difference between the two will be clear. Furthermore, most of the kSZ signal should be strongly correlated with the thermal SZ effect. However, the kSZ signal will be a large source of contamination in the central regions, with a significant source of noise coming from bulk motions within the cluster due to objects that have recently been accreted.

Seljak and Zaldarriaga (2000) considered idealized spherical clusters lensing a pure temperature gradient.

They also provided an extensive list of potential systematic effects which must be overcome to observe the signal. In the space of three years, the sensitivity and resolution of envisioned microwave background measurements have increased dramatically, prompting a more detailed assessment of the cluster lensing signal. In this paper, we use model mass distributions from clusters in a cosmological N-body simulation to lens a background Gaussian temperature field constructed from the temperature power spectrum in a realistic cosmological model. The cluster lensing signal is clear in the resulting map. Section II displays how the signal varies with cluster mass and cluster location on the sky, and Section III considers how well the cluster lensing signal can be inferred from an ideal map using a correlation function technique for estimating the unlensed temperature distribution. More elaborate model-fitting techniques are likely straightforward but beyond the scope of the paper, requiring explicit and careful considerations of specific instruments and observing strategies. Finally, we discuss potential advantages and systematic limitations of this method for cluster mass determination in the context of realistic experiments.

2. ORDER-OF-MAGNITUDE ESTIMATES

The root-mean-square temperature gradient in the primary microwave background fluctuations is around 12 μK per arcminute for standard cosmological models consistent with the measured microwave power spectrum; the magnitude of the lensing signal is on the order of the local temperature gradient times the characteristic angular deflection. Typical deflection angles (roughly the cluster gravitational potential in units of c^2, $\Phi/c^2 \simeq 10^{-4}$) are on the order of tens of arcseconds. The fractional perturbation due to lensing is therefore on the order of a few μK.

This is at least an order of magnitude larger than perturbations due to the transverse velocity of the cluster (Birkinshaw & Gull 1983), which is on the order of the cluster potential Φ/c^2 times the transverse velocity v_{trans}/c. Typical peculiar velocities are a few hundred km/s, so this term should be at the level of roughly 0.1 μK. Similarly, anisotropy imprinted from the cluster potential changing over the photon travel time (the Integrated Sachs-Wolfe effect in the non-linear regime) should be roughly given by the potential times the photon travel time relative to the dynamical time. With travel times on the order of 1 Myr and dynamical times on the order of 1 Gyr this term should be comparable to the transverse velocity effects but well below the expected level of lensing effects. Therefore, the signatures of moving or dynamically evolving clusters will be strongly suppressed compared to lensing of the CMB, even if the thermal and kinematic SZ effects can be efficiently removed.

As discussed below, the kinematic SZ effect is also expected to be on the order of a few μK, with a similar spectral dependence to gravitational lensing. These two signals must be separated via their spatial morphology or other techniques.

3. LENSED MAPS

Figure 1 displays the lensing of a pure temperature gradient by a numerically simulated cluster of galaxies of mass $M = 6h^{-1} \times 10^{14} M_\odot$ at a redshift of $z = 0.5$, while Fig. 2 shows the same cluster lensing two realizations of a Gaussian random temperature field with the power spectrum of the microwave background for a flat ΛCDM cosmological model with $n = 1$, $h = 0.7$, $\Omega_b h^2 = 0.024$, and $\Omega_\Lambda = 0.7$. Equal-temperature contours are plotted at 5 μK separations as light dotted lines. To display the lensing signal more clearly, we then high-pass filter the map with a 3-arcminute filter scale. The temperature contours of the filtered map are plotted at 0.5 μK separations as heavy lines.

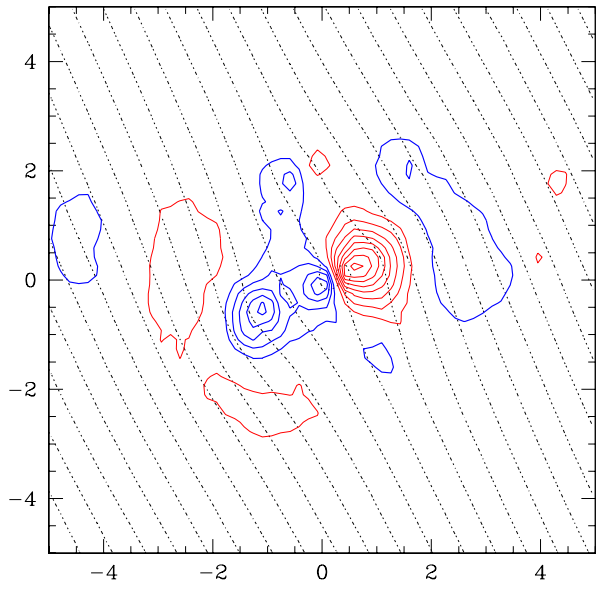

FIG. 1.— Gravitational lensing of a pure background gradient of 15 μK per arcminute by a galaxy cluster of mass $7 \times 10^{14} h^{-1} M\odot$ extracted from a numerical simulation. Background contours are spaced by 5 μK and show the unfiltered lensed signal, while solid contours, spaced by 0.5 μK, show maps that have been high-pass filtered, with all $k \lesssim 1150$ ($\ell \lesssim 7200$) removed. Each image is $5' \times 5'$ and does not include kinematic SZ effects. Blue (thick) contours indicate positive temperature differences, while red (thin) contours indicate negative values.

The cluster is drawn from the VIRGO[1] simulations (da Silva et al. 2000). Outputs (including gas) were available at $z = 0$, and for our lensing calculation we artificially placed the simulation volume at $z = 0.5$. To be conservative, we did not scale the box size to account for the expansion of the universe between $z = 0.5$ and $z = 0$. This scaling would lead to an overestimate of the central concentration of virialized objects at $z = 0.5$ in the simulation, and therefore an overestimate of the lensing signature. The box was translated such that a massive cluster was at the center of the projected mass distribution, and the dark matter distribution was projected onto a 2048×2048 grid using a simple nearest grid point method. The gas was smoothed (in projection) over the mean distance to the 24th nearest neighbor assuming a uniform disk smoothing kernel. The resulting surface mass density map was used to generate deflection maps with resolution of roughly 10", using an FFT

[1] http://virgo.sussex.ac.uk

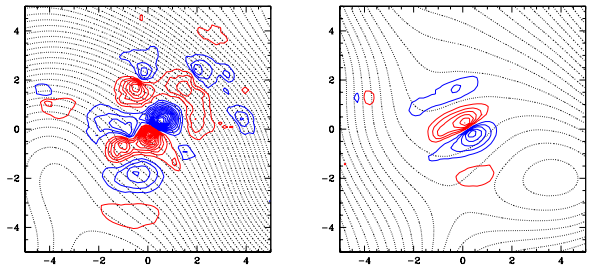

FIG. 2.— Same as Fig. 1, except that the cluster is lensing two different realizations of a CMB sky.

method.

We compute the reduced angular deflection vector due to the cluster mass distribution in the thin-lens approximation,

$$\alpha(\mathbf{x}) = \frac{1}{\pi}\int \kappa(\mathbf{x}')\frac{\mathbf{x}-\mathbf{x}'}{|\mathbf{x}-\mathbf{x}'|^2}d\mathbf{x}' \quad (1)$$

where $\mathbf{x}$ is a 2-dimensional vector describing the angular position on the sky, $\kappa(\mathbf{x})$ is the projected convergence related to the surface mass density Σ by

$$\kappa(\mathbf{x}) = \frac{4\pi G}{c^2}\frac{D_{\rm d}D_{\rm ds}}{D_{\rm s}}\Sigma(\mathbf{x}) \quad (2)$$

with $D_{\rm d}$, $D_{\rm s}$, and $D_{\rm ds}$ the angular diameter distances from the observer to the lens, the observer to the source, and the lens to the source, respectively. The actual deflection vector $\hat{\alpha}$ is related to the reduced deflection by the distance scaling $\alpha = (D_{\rm ds}/D_{\rm s})\hat{\alpha}$. (See, e.g., Schneider et al. (1992) for a detailed exposition of standard gravitational lensing theory.)

A lensed map can be constructed from an unlensed background map and a surface mass distribution $\Sigma(\mathbf{x})$ by solving the lens equation

$$\beta(\mathbf{x}) = \mathbf{x} - \alpha(\mathbf{x}) \quad (3)$$

where β is the source position in the image plane. For a source covering the entire sky like the microwave background, the lens equation is straightforward to solve by pixellating the image plane, then using the displacement vector to map each point in the image plane to a point of the source plane, then assign the source temperature at that point to the original point in the image plane. The resulting lensed maps in Fig. 1 represent the signal an ideal experiment with very high angular resolution and sensitivity might measure.

The CMB maps were generated using a CMB power spectrum generated by CMBFast[2] (Seljak & Zaldarriaga 1996). To be conservative, we use the lensed power spectrum, which has slightly more power on small scales, but assume the underlying CMB anisotropies are a Gaussian random field. We construct unlensed maps over small regions of sky using the flat sky approximation.

The cluster lensing signals are obvious in the filtered maps. It is clear that lensing induces structure in the maps on significantly smaller scales than those on which the microwave background has significant temperature fluctuations. For a cluster situated in front of a region of the microwave background which is approximately a temperature gradient, lensing produces a characteristic dipole-like pattern, with a cool and a hot peak. The peak-to-peak amplitude is proportional to the gradient magnitude, but is generally on the order of 1 to 10 μK; the angular separation of the peaks is on the order of an arcminute, with noticeable lensing effects out to radii of several arcminutes. Also note that a vector from the hot to the cool lensing peak must be in the direction of the local CMB gradient: this distinctive signature can be used to discriminate between a lensing signal and other effects local to the galaxy cluster, which will be physically uncorrelated with the microwave background.

The gross features of the cluster lensing signal depend on cluster mass, redshift, and sky location. The lensing effect depends on the angular diameter distance to the cluster; for massive clusters which are distant enough that their angular size is on the order of an arcminute, their angular diameter distance is only a weak function of redshift. The lensing deflection depends primarily on the total mass of the cluster. The other crucial factor in the cluster lensing pattern is sky position: the amplitude of the lensing signal is proportional to the local background temperature gradient. To extract mass information about the cluster, we must be able to infer the unlensed background temperature pattern. This is easiest when the cluster is situated in a sky region which has a fairly uniform temperature gradient; in this case the characteristic dipole lensing pattern is produced. If the cluster is located in a region of the sky where the temperature field is near an extremum, or where the isotemperature contours are strongly curved, extraction of the lensing mass is more uncertain, because the unlensed temperature field is not as well constrained by the lensed map.

Figure 3 shows clusters with a range of different masses lensing the microwave background. Here the simulated lensing mass distribution is a cubic volume $100h^{-1}$ Mpc on a side drawn from the VIRGO simulations, placed at a redshift of $z = 0.5$. Both the amplitude of the lensing peaks and their angular separation increase with cluster mass. To gauge the effects of sky position, we have outlined with a square the location of all clusters in the simulated mass distribution with $M > 10^{14}\,M_\odot$. Some marked clusters do not obviously correspond to clean features in the filtered map, indicating that the lensing signature is very difficult to observe at these positions. Roughly half of the $10^{14}\,M_\odot$ clusters in Fig. 3 are in sky positions leading to appreciable lensing signals. As a rule of thumb, the lensing signal will be easiest to estimate when $|\nabla T|$ is large and $\nabla^2 T$ is small. At the same time, occasional less massive objects that are particularly well-placed at the positions of strong gradients display clear lensing signatures, as with the cluster near $(-30', 5')$. Note that the positions of all clusters will be known from their thermal Sunyaev-Zeldovich distortions, which are at least an order of magnitude larger than the lensing signature.

In Figure 4 we show the problems that can be introduced by significant substructure in the kSZ signal. This case is chosen as an unfavorable kSZ signal, although it could be even less favorable if aligned exactly with the gradient. Some of the kSZ is removed by selecting only that component that is anti-symmetric around the clus-

[2] www.cmbfast.org

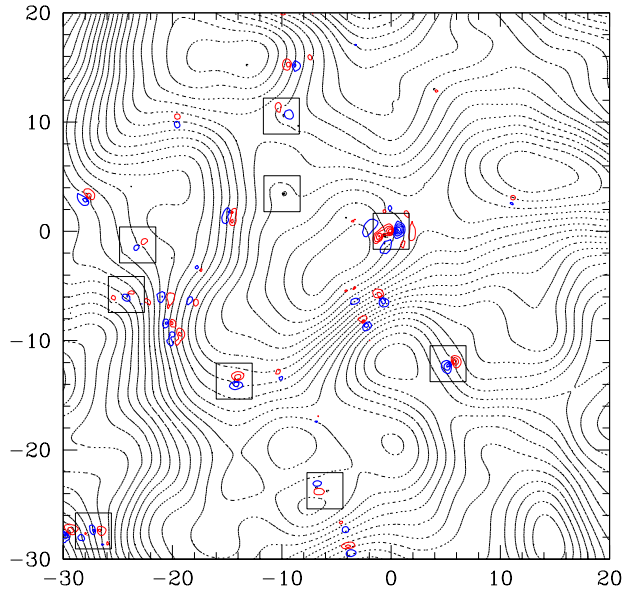

FIG. 3.— $50' \times 50'$ field showing several clusters lensing the CMB. All positions of clusters with masses above $10^{14}h^{-1}M_\odot$ are shown as open squares in the map, and background dotted contours are spaced every 15 μK. Solid contours show a high-pass filtered map with 0.5 μK temperature contours, as in Fig. 1.

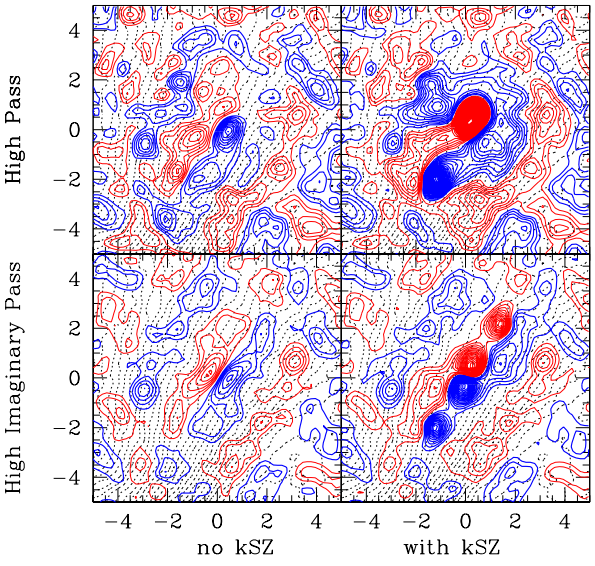

FIG. 4.— Effects of kinetic SZ signal: left two panels show case of no kSZ, right two panels include a large contaminating kSZ signal. Top panels show a simple high-pass filter, as in figure 1, while bottom two panels show the effect of a high-pass filter that has also selected the component that is anti-symmetric around the cluster center (i.e., the imaginary part of the Fourier transform).

ter center (as the lensing signal should be). Along the direction of the gradient, it is still possible to see the characteristic lensing distortion, but it is clear that the central region will be useless for the purposes of lensing reconstructions. We emphasize that this was not selected as a typical contamination, and the simulation physics (no feedback or preheating) led to gas cores that are much more concentrated than in observed clusters.

4. DEFLECTION ESTIMATION

The maps in the previous section make clear that in many cases (but not all), some estimate of cluster mass within a certain radius can be made from the pattern of lensing in the microwave background. It is likely that some kind of model fitting for both the cluster mass profile and the unlensed temperature map will give the most accurate cluster mass recovery, but a complete parametric study is beyond the scope of this paper. Here we present a crude technique for estimating the lensing deflection in the inner region of the cluster which works well in many cases. This deflection angle can then be used as a constraint on the mass distribution.

4.1. *Wiener Estimation of Unlensed Background*

For the case of a source intensity distribution which is a pure gradient, it is straightforward to estimate the lensing deflection in the direction along the temperature gradient. At sufficiently large distances from the cluster center, the background gradient will be clear and can be robustly estimated. For the case of the microwave background, a pure gradient is generally *not* a good description of the background temperature distribution on scales of a few arcminutes over which lensing deflections are significant. However, the background temperature distribution is close to a gaussian random field, and the statistical nature of this distribution can be used to estimate the unlensed background temperature distribution in the region of a cluster: we mask out the central regions of the image, where lensing is known to be important, and interpolate an approximate unlensed temperature distribution using the region that is more than a few arcminutes away from the center.

The most reliable method we found is Wiener interpolation. We assume that the correlation function of the microwave background temperature is known from power spectrum measurements. Then we have a good estimate of $\langle T_i T_j \rangle = C(|\theta_i - \theta_j|) \equiv C_{ij}$, the mean product of temperatures at two points θ_i and θ_j in the map; here $C(\theta)$ is the temperature correlation function for two points with angular separation θ. The matrix $\mathbf{C}$ is just the theoretical gaussian random correlation matrix constructed from the power spectrum. Given accurate estimates of the temperature map outside the cluster region, we can use these correlation functions to interpolate across the cluster.

The pixels of some observed map can be viewed as a single data vector $\mathbf{d}$. We then form the noise-weighted covariance matrix $\mathbf{D}$: this covariance matrix includes the theoretical covariance $\mathbf{C}$ plus the covariance arising from pixel noise. We mask out given pixels in the region of a cluster by setting the diagonal elements of $\mathbf{D}$ corresponding to those pixels to a value which is large compared to the other elements of $\mathbf{D}$. We then estimate the temperature map $\mathbf{t_{est}}$ defined by the theoretical correlation function which matches the measured pixels in the region ouside the cluster as $\mathbf{t_{est}} = \mathbf{C}\mathbf{D}^{-1}\mathbf{d}$. This construction requires inversion of a large matrix. For a map with $N \times N$ pixels, the computation of the inverse covariance matrix scales as N^6, but pixels well beyond the

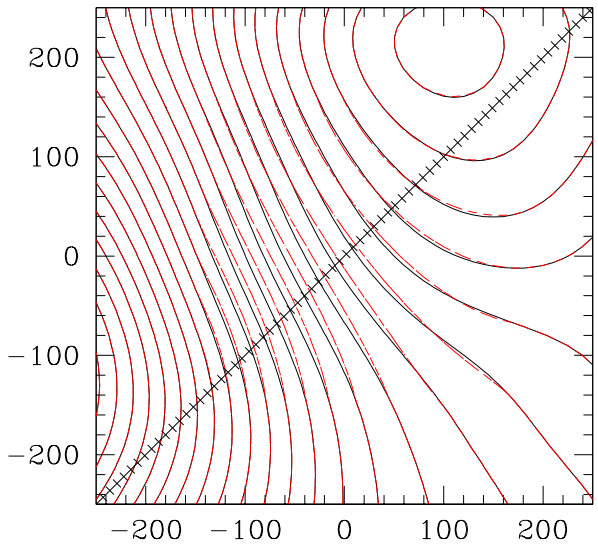

FIG. 5.— Reconstruction of unlensed CMB background field using Wiener interpolation. The axes are in arcseconds, and the diagonal line is marked in units of 5 arcseconds; temperature contours are spaced at 5 μK intervals. Reconstruction of the central $5' \times 5'$ section of the map is done using the displayed map region with an effective pixel scale of 10". Solid lines show the input map, dashed lines show the reconstructed map.

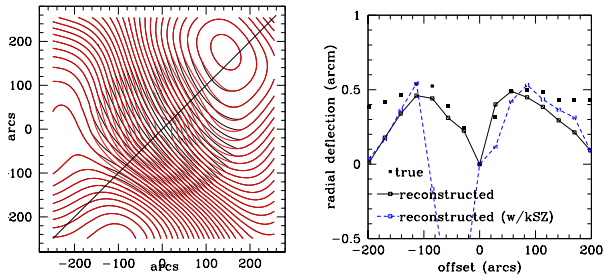

FIG. 6.— Reconstruction of lensing deflection angle. Left panel shows lensed and reconstructed unlensed CMB map; the axes are in arcseconds. The diagonal line shows the slice that was used to reconstruct the radial deflection angle shown in the right panel. The solid curve shows the reconstruction in the case where the kSZ can be perfectly removed, while the dashed line shows the deflection estimate when no kSZ has been removed.

cluster region do not contribute much to the cluster region. Also, note that this inversion must be done only once for a given microwave background power spectrum, pixel scale, and mask geometry.

As a verification of the method, we start with a CMB realization (with no cluster lensing), cut out the central 8' and use the Wiener method to reconstruct the missing pixels. Results are shown in Figure 5. The reconstruction is not perfect, but the reconstruction errors are on the order of 5", small compared to typical lensing deflection angles of 30-40". For Fig. 5, we used a map that was 64×64 pixels with a 10" pixel scale. This reconstruction took a few minutes on a desktop computer without any particular optimization effort.

We also experimented with fitting a simple gradient or two-dimensional splines of varying stiffnesses, with varying degrees of success on a case-by-case basis. For the Wiener interpolation technique, assuming the outer regions are unaffected by lensing introduces an unnatural boundary condition, so an iterative approach would improve this estimate. Ultimately, a simultaneous fit for the unlensed CMB distribution, kinematic SZ, and deflection angle will be required for the most reliable constraints, and will use the corresponding thermal SZ map to provide a rough template for the kinematic SZ signal.

We note that the Wiener estimation technique provides a general method for testing Gaussianity of the microwave background temperature distribution.

4.2. *Deflection Angle Reconstruction*

Applying the Wiener estimation method, we show the reconstructed deflection angle along a slice through the cluster center in Fig. 6. At the edge of the masked region, the deflection goes to zero by construction; it may be useful to employ an iterative approach to more accurately reconstruct the outer regions. The inner few arcminutes are accurately reconstructed, providing information on the cluster mass distribution.

A cluster will produce a second microwave background distortion with a near-blackbody spectrum in addition to lensing, namely the kinematic Sunyaev-Zeldovich (kSZ) effect (Sunyaev & Zel'dovich 1972). This distortion arises from photons scattered by the cluster gas moving with some bulk velocity relative to the microwave background rest frame. If clusters were balls of gas with no significant internal motions, the result would be either a positive or negative temperature distortion proportional to the gas density profile, for clusters with radial velocities toward or away from the observer. This is easily distinguishable from the dipole-like pattern induced by lensing. Furthermore, this spatial pattern would be matched by the thermal SZ signature, and could be projected out. However, actual clusters possess significant internal coherent bulk velocities, particularly for higher-redshift clusters undergoing frequent mergers, and these internal velocities result in more complex kSZ distortions (see, e.g., Nagai et al. (2003)). Occasionally, the resulting kSZ maps can even mimic the dipole-like pattern seen in lensing, although alignment with the temperature gradient would be purely coincidental.

The degree to which the kSZ effect will degrade mass estimates will vary between individual clusters. Generally, the region of significant kSZ distortion is more spatially concentrated than the lensing signal, and will have some correlation with the thermal SZ distortion since both scale with the cluster's total optical depth. Figure 6 also shows recovered deflection angles when the kSZ effect is included. Clearly, the lensing reconstruction is seriously degraded in the central cluster region where the kSZ signal is comparable to the lensing signal, but for regions further from the center, the kSZ signal does not alter the reconstruction. In practice, the temperature fluctuations in an annulus from 1' to 3' away from the cluster will provide most of the information about lensing deflections.

We have not included residual noise from large scale structure (Vishniac 1987), which should be at the level of roughly 1 μK at the resolution of these maps. While

this noise makes maps less visually appealing at the lowest contour levels, it does not quantitatively affect the ability to reconstruct deflection angles. Assuming typical gradients of 12 μK per arcminute, noise at the level of 1 μK corresponds to fluctuations at the level of 5" in the deflection angle.

All of the above analysis has been for idealized maps, which here is equivalent to an angular resolution of $10''$ and noise levels below 1 μK per resolution element. The next generation of microwave background maps at small scales (e.g., Atacama Cosmology Telescope; ACT Kosowsky (2003) or South Pole Telescope; SPT) will attain resolutions of roughly 1' and noise levels of a few μK per resolution element. The ability to detect actual lensing deflections at these resolutions and sensitivities will be lower than presented here; quantitative analysis of how much the signal is degraded is ongoing. Eventually, the Atacama Large Millimeter Array, ALMA[3] (Wootten 2002), will have both the sensitivity and resolution to make the kinds of maps displayed in this paper, provided systematic errors can be controlled well enough to allow reliable imaging of more than ten square arcminutes (requiring a large mosaic).

4.3. *Mass From Deflection*

In an ideal case, lensing of the microwave background determines the component of the deflection angle in the direction of the local temperature gradient. In principle, this is not sufficient information to determine the mass distribution. The deflection $\alpha(\mathbf{x})$ can be expressed as the gradient of a lensing potential, $\alpha = \nabla\psi$; thus the deflection field is curl-free, $\nabla \times \alpha = 0$. Thus if we infer α_x from a map, in principle this determines $\partial\alpha_y/\partial x$ as well (though of course no practical algorithm should differentiate measured data!). However, we cannot obtain α_y itself by integrating with respect to x, because a different integration constant obtains for each value of y. So we cannot recover the complete deflection angle α nor the convergence (mass density) $2\kappa = \nabla \cdot \alpha$, but rather one component of the deflection and the derivative of its orthogonal component.

In practice, a number of other reasonable assumptions or constraints can be imposed. Assuming the deflection to be zero beyond some given radius will break the degeneracy while biasing the cluster mass estimate. The assumption of a spherically symmetric lens will also break the degeneracy; more generally, assuming almost any parametric form for the lens will largely lift the degeneracy.

4.4. *Errors in Cluster Catalogs*

So far we have discussed galaxy clusters individually. Future high-resolution microwave maps will yield samples of hundreds to thousands of galaxy clusters selected by their thermal SZ spectral distortions. The lensing signals in these samples can be used to probe the cluster mass distribution in a statistical sense. In this case, it is important to distinguish statistical errors, which will average out in a large cluster sample, from systematic ones which will not.

The major sources of error affecting the lensing observations and analyses described here are residual uncertainties from projecting out the thermal SZ spectral distortions and other non-blackbody foreground components like dust or point sources; separation of the kSZ signal from the lensing plus background CMB signals; errors in reconstructing the deflection map from the lensed CMB map; and other neglected sources of signal like the moving cluster effect. In order for an error to have a systematic impact on lensing mass estimates, it must correlate with the cluster lensing signal, which is aligned with the local temperature gradient. This means that no foreground emission is likely to contribute any systematic error to the lensing signal. The separation of the thermal SZ signal is also unlikely to give any systematic error, because of its roughly symmetric shape. The moving cluster effect is both negligibly small for any single cluster and also uncorrelated with the background temperature gradient so it will not give any systematic effect over a significant survey area (i.e., a few square degrees). The kinematic SZ effect can coincidentally mimic the lensing signal to some extent in the case of a cluster undergoing a merger, but the dipole-like morphology of the signal will only be aligned with the background temperature gradient by coincidence in a small fraction of these merging clusters; also any kinematic SZ dipole-shaped signature will be over smaller angular scales than the lensing signal and will mostly be eliminated by masking out the central portion of the cluster.

The only clear potential systematic error arises from the technique used to separate the lensing signal and the background fluctuations. In our sample technique in this paper, for example, we reconstruct the deflection over some finite-area region around the cluster, assuming zero deflection at the edges of the region. This leads to a systematic underestimate of the deflection in the outer parts of the cluster, as seen in Fig. 6. The extent to which this systematic error biases ultimate mass estimates depends on the details of the method used to reconstruct the deflection. This bias depends primarily on the shape of the background fluctuations, and for a given reconstruction technique can probably be modelled with a fair degree of certainty. Detailed estimates of the size of this systematic error when constructing statistical estimates from cluster catalogs is beyond the scope of this paper.

5. DISCUSSION

Cluster mass estimates based on the gas distribution, such as those extracted from X-ray temperature maps or from the Sunyaev-Zeldovich effect, have intrinsic uncertainties arising from the detailed relationship between the gas distribution and the total mass distribution, particularly at higher redshifts when clusters undergo frequent mergers. The only direct way to measure cluster masses is through gravitational lensing. Strong and weak lensing of background galaxies by a cluster give measurements of the shear field induced by the cluster mass distribution, and elaborate techniques have been developed to reconstruct an estimated mass distribution from lensing observations (Kaiser & Squires 1993; Squires & Kaiser 1996). A number of cluster masses have been measured this way (Fisher & Tyson 1997; King et al. 2002; Tyson et al. 1998; Wittman et al. 2001).

However, cluster mass determination via lensing of background galaxies has a number of limitations. At

[3] www.alma.nrao.edu

usual magnitude limits, most clusters do not exhibit the arcs of strongly lensed background galaxies, which arise due to chance alignment of the cluster and background galaxy. Mass measurements for large samples of galaxy clusters thus cannot rely on strong lensing as a primary tool. Weak lensing of faint background galaxies provides a more generic signal. But weak lensing has a number of difficult systematic considerations: (1) Orientations of background galaxies possess some degree of intrinsic alignment, which can bias the lensing signal (Brown et al. 2002; Catelan et al. 2001; Crittenden et al. 2001; Croft & Metzler 2001; Heavens et al. 2000; Pen et al. 2000). (2) The redshift distribution of background galaxies is generally not well determined, and photometric redshift distributions may induce significant systematic errors (McKay et al. 2002; Sheldon et al. 2003; Smith et al. 2001). (3) The lensing signal becomes weaker for higher cluster redshifts because fewer background galaxies are behind high-redshift clusters. (4) At a given exposure depth, weak lensing measurements are limited by shot noise due to a finite number of background galaxies.

Lensing of the microwave background ameliorates these limitations. The photons all originate from a single, precisely-determined redshift. and this surface of last scattering is well behind any cluster, simplifying the redshift dependence of the lensing signal Furthermore, given sufficient resolution, the lensed temperature pattern can be probed with arbitrary accuracy, circumventing the shot noise limits. An additional potential advantage, pointed out by Seljak and Zaldarriaga (2000), is that deflection angle drops off more slowly with distance from the cluster than does shear. However, as radius increases, the comparatively larger lensing signal is counteracted by the larger noise (arising from the primary CMB anisotropies) from uncertain knowledge of the unlensed background; in practice this advantage over weak lensing is uncertain.

The microwave background lensing signal will have its own systematic limitations. Foremost among these are the contribution of the kSZ signal and our limited knowledge about the underlying primordial temperature fluctuation pattern. As illustrated here, the impact of each of these varies from cluster to cluster. It is safe to say that some non-negligible fraction of clusters will be good candidates for lensing mass determinations, due to their location in front of a favorable area of temperature fluctuations and their lack of significant internal bulk velocities producing a complicated kSZ contribution. Also, which clusters will provide the most reliable lensing deflection determination will be evident from the maps themselves.

Finally, any lensing mass estimate does not probe only the cluster mass, but rather all of the mass projected along the line of sight to the cluster. Generally, this total projected mass is dominated by the galaxy cluster mass, but other masses will lead to a small systematic bias towards overestimating cluster masses. This can be addressed by comparing observations to full cosmological simulations instead of to a simple cluster mass distribution (Chen et al. 2003). Note that weak and strong lensing of background galaxies also suffer from this difficulty, although the larger redshift of the microwave background makes the effect somewhat more important. The linear contribution due to large scale structure has been crudely included by our use of the lensed CMB power spectrum, but this does not adequately include the effects of non-Gaussianity and non-linearity.

Of course, the usual slew of difficulties in making accurate, high-resolution and high-sensitivity microwave background maps will also need to be overcome, including foreground emission, point sources, and the cluster's comparatively large thermal Sunyaev-Zeldovich distortion. Confusion-limited infrared point sources, in particular, will be a serious problem at arcminute resolutions (Blain 1998; Borys et al. 2003; Knox et al. 2003). The cluster thermal SZ effect can be minimized by observing near the frequency null around 220 GHz. Thermal SZ and foreground separation at the μK level will require multi-frequency observations, although both will be uncorrelated with the specific lensing temperature distortions around clusters. Accurate measurement of lensing signals with maximum amplitudes of a few μK in individual clusters will likely require sub-arcminute resolution observations over a range of frequencies by an instrument like ALMA, and may be marginally detectable with ACT or SPT.

Lensing of the CMB polarization fluctuations should be less susceptible to many sources of confusion than lensing of the temperature fluctuations considered in this paper: the kSZ and thermal SZ polarization fluctuations are significantly smaller than the corresponding temperature fluctuations, and infrared point sources, which are actually the total dust emission from high-redshift galaxies, are likely to show little polarized emission. Furthermore, the primary CMB polarization pattern on small scales will have a particular spatial property (curl-free) that is violated in the presence of lensing (Kamionkowski et al. 1997; Zaldarriaga & Seljak 1997), providing a "smoking gun" of the presence of lensing distortions. If the systematic limitations to measuring lensing deflections from temperature maps prove difficult to overcome, polarization maps provide a viable alternative (although they require still greater experimental sensitivity due to the smaller polarization amplitude in the primary microwave background fluctuations).

The importance of constraining galaxy cluster masses hardly needs to be emphasized. The number density of clusters of a given mass as a function of redshift is a highly sensitive probe of the growth rate of structure, and in principle could strongly constrain the scale factor evolution at recent cosmological epochs (Haiman et al. 2001). The problem is that traditional cluster observations in optical and X-ray bands, or measurements of the Sunyaev-Zeldovich distortion, measure the distribution of baryons in the cluster, not its total mass. Connecting the distribution of baryons and dark matter in clusters is a difficult and complex problem, providing many possibilities for systematic errors in cluster mass estimates, particularly at larger redshifts where clusters are further from dynamical equilibrium due to frequent merging. Lensing measurements appear to be the only route to a direct, reliable cluster mass estimate. A clear understanding and characterization of cluster lensing is also essential for probing the cluster kinematic SZ signal (Holder 2003; Nagai et al. 2003), where the lensing acts as an unwanted complication. We hope that the images and arguments in this paper convincingly demonstrate that microwave background lensing is a viable alterna-

tive to weak lensing of background galaxies for learning about the distribution of mass in galaxy clusters.

Note: since submission of this work, two noteworthy papers of relevance have appeared in the literature (Dodelson 2004; Vale et al. 2004). These works confirm the results presented here and present interesting discussions of other important issues and directions for lensing of the CMB by galaxy clusters.

This work has been partially supported by NASA Space Astrophysics Research and Analysis grant NAG5-10110 at Rutgers. A.K. is a Cottrell Scholar of the Research Corporation, and G.H. is supported by the W.M. Keck Foundation.

REFERENCES

Bartelmann, M. 2003, astro-ph/0304162
Birkinshaw, M., & Gull, S. F. 1983, Nature, 302, 315
Blain, A. W. 1998, MNRAS, 297, 502
Borys, C., Chapman, S., Halpern, M., & Scott, D. 2003, MNRAS, 344, 385
Brown, M., et al. 2002, MNRAS, 333, 501
Catelan, P., Kamionkowski, M., & Blandford, R. 2001, MNRAS, 323, 713
Chen, J., Kravtsov, A., & Keeton, C. 2003, ApJ, 592, 24
Cooray, A. 2003, ApJ, 596, L127
Crittenden, R., et al. 2001, ApJ, 559, 552
Croft, R., & Metzler, C. 2001, ApJ, 545, 561
da Silva, A., et al. 2000, MNRAS, 317, 37
Dodelson, S., & Starkman, G. D. 2003, astro-ph/0305467
Dodelson, S., 2004, preprint, astro-ph/0402314
Fisher, P., & Tyson, J. 1997, ApJ, 114, 14
Haiman, Z., Mohr, J. J., & Holder, G. P. 2001, ApJ, 553, 545
Heavens, A., Refregier, A., & Heymans, C. 2000, MNRAS, 319, 649
Hirata, C., & Seljak, U. 2003, Phys. Rev. D, 67, 043001
Holder, G. P. 2003, ApJ, in press, astro-ph/0207600
Kaiser, N., & Squires, G. 1993, ApJ, 404, 441
Kamionkowski, M., Kosowsky, A., & Stebbins, A. 1997, Phys. Rev. D, 55, 7368
Kesden, M., Cooray, A., & Kamionkowski, M. 2003, Phys. Rev. D, 67, 123507
King, L., et al. 2002, A&A, 385, L5
Knox, L., Holder, G., & Church, S. 2003, ApJ, submitted
Kosowsky, A. 2003, New Astron. Rev., 47, 939
McKay, T., et al. 2002, astro-ph/0108013
Nagai, D., Kravtsov, A., & Kosowsky, A. 2003, ApJ, 587, 524
Okamoto, T., & Hu, W. 2002, ApJ, 574, 566
—. 2003, Phys. Rev. D, 67, 83002
Pen, U., Lee, J., & Seljak, U. 2000, ApJ, 543, L107
Schneider, P., Ehlers, J., & Falco, E. 1992, Gravitational Lensing (Springer-Verlag)
Seljak, U., & Zaldarriaga, M. 1996, ApJ, 469, 437
—. 2000, ApJ, 538, 57
Sheldon, E., et al. 2003, astro-ph/0312036
Smith, D. R., Bernstein, G. M., Fischer, P., & Jarvis, M. 2001, ApJ, 551, 643
Squires, G., & Kaiser, N. 1996, ApJ, 473, 65
Sunyaev, R. A., & Zel'dovich, Y. B. 1972, Comments Astrophys. Space Phys., 4, 173
Tyson, J., Kochanski, G., & Dell'Antonio, I. 1998, ApJ, 498, L107
Vale, C., Amblard, A., & White, M. 2004, New Astronomy, in press astro-ph/0403075
Vishniac, E. T. 1987, ApJ, 322, 597
Wittman, D., et al. 2001, ApJ, 557, L89
Wootten, A. 2002, The Atacama Large Millimeter Array (ALMA), Tech. rep., NRAO report 02133
Zaldarriaga, M., & Seljak, U. 1997, Phys. Rev. D, 55, 1830